



|                  |  |
|------------------|--|
| Title            | Calmodulin-dependent protein kinase II (CaMKII) mediates radiation-induced mitochondrial fission by regulating the phosphorylation of dynamin-related protein 1 (Drp1) at serine 616                     |
| Author(s)        | Bo, Tomoki; Yamamori, Tohru; Suzuki, Motofumi; Sakai, Yuri; Yamamoto, Kumiko; Inanami, Osamu   |
| Citation         | Biochemical and biophysical research communications, 295(2), 1601-1607<br><a href="https://doi.org/10.1016/j.bbrc.2017.12.012">https://doi.org/10.1016/j.bbrc.2017.12.012</a>                            |
| Issue Date       | 2018-01-08   |
| Doc URL          | <a href="http://hdl.handle.net/2115/72273">http://hdl.handle.net/2115/72273</a>  |
| Rights           | © 2018. This manuscript version is made available under the CC-BY-NC-ND 4.0 license<br><a href="http://creativecommons.org/licenses/by-nc-nd/4.0/">http://creativecommons.org/licenses/by-nc-nd/4.0/</a> |
| Rights(URL)      | <a href="http://creativecommons.org/licenses/by-nc-nd/4.0/">http://creativecommons.org/licenses/by-nc-nd/4.0/</a>  |
| Type             | article (author version)   |
| File Information | BBRC.pdf   |



[Instructions for use](#)

**Calmodulin-dependent protein kinase II (CaMKII) mediates radiation-induced mitochondrial fission by regulating the phosphorylation of dynamin-related protein 1 (Drp1) at serine 616**

Tomoki Bo<sup>a</sup>, Tohru Yamamori<sup>a\*</sup>, Motofumi Suzuki<sup>b</sup>, Yuri Sakai<sup>a</sup>, Kumiko Yamamoto<sup>a</sup>, and Osamu Inanami<sup>a\*</sup>

<sup>a</sup>Laboratory of Radiation Biology, Department of Applied Veterinary Sciences, Faculty of Veterinary Medicine, Hokkaido University, Sapporo, Japan

<sup>b</sup>Radiation and Cancer Biology Team, National Institutes for Quantum and Radiobiological Science and Technology, Chiba, Japan

\*Corresponding authors: Dr. Tohru Yamamori and Prof. Osamu Inanami

Address: Kita 18, Nishi 9, Kita-ku, Sapporo, Hokkaido 060-0818, Japan

Tel: +81-11-706-5236 (TY), +81-11-706-5235 (OI)

Fax: +81-11-706-7373

E-mail: yamamorit@vetmed.hokudai.ac.jp (TY), inanami@vetmed.hokudai.ac.jp (OI)

## **ABSTRACT**

Mitochondrial dynamics has been suggested to be indispensable for the maintenance of cellular quality and function in response to various stresses. While ionizing radiation (IR) elicits mitochondrial fission mediated by the mitochondrial fission protein dynamin-related protein 1 (Drp1), it remains unclear how IR promotes Drp1 activation and subsequent mitochondrial fission. Therefore, we conducted this study to answer these questions. First, we found that X-irradiation triggered Drp1 phosphorylation at serine 616 (S616), but not at serine 637 (S637). Reconstitution analysis revealed that introduction of WT Drp1 recovered radiation-induced mitochondrial fission, which was lost in Drp1-deficient cells. Compared with the cells transfected with WT or S637A Drp1, the mitochondrial shape change after irradiation was mitigated in S616A Drp1-introduced cells. Furthermore, inhibition of CaMKII significantly suppressed Drp1 S616 phosphorylation and mitochondria fission induced by IR. These results suggest that Drp1 phosphorylation at S616, but not at S637, is prerequisite for radiation-induced mitochondrial fission and that CaMKII regulates Drp1 phosphorylation at S616 after irradiation.

*Keywords:* CaMKII, Drp1, Ionizing radiation, Mitochondrial dynamics, Phosphorylation

*Abbreviations:* CaMKII, calmodulin-dependent protein kinase II; cPKC, conventional protein kinase C; CDK1, cyclin-dependent kinase 1; Drp1, dynamin-related protein 1; GFX, GF109203X; Gö, Gö6976; IR, ionizing radiation; Fis1, mitochondrial fission

protein 1; Mff, mitochondrial fission factor; Mfn1/2, mitofusin 1/2; Opa1, optic atrophy 1; PMA, phorbol 12-myristate 13-acetate; PTMs, posttranslational modifications; PKC $\delta$ , protein kinase C  $\delta$ ; S616, serine 616; S637, serine 637; S693, serine 693.

## **INTRODUCTION**

Mitochondria are dynamic organelles that undergo continuous fission and fusion cycles. Previous studies have shown that the balance of fission and fusion, called mitochondrial dynamics, is essential to maintain cellular function in response to various stresses. Mitochondrial dynamics is the process regulated by a number of proteins [1]. Mitofusin 1/2 (Mfn1/2) and optic atrophy 1 (Opa1) are the main regulatory proteins for mitochondrial fission. While Mfn1/2 localize on the outer mitochondrial membrane and promote fusion of the outer mitochondrial membranes, Opa1 localizes on the inner mitochondrial membrane and fuses the inner mitochondrial membranes. On the other hand, mitochondrial fission is mediated by dynamin-related protein 1 (Drp1) and its adapter proteins including mitochondrial fission protein 1 (Fis1) and mitochondrial fission factor (Mff). Drp1 is a cytosolic protein that, on activation, translocates to the outer mitochondrial membrane and docks on the adapter proteins. On the scission sites, Drp1 forms ring-like structures that constrict and eventually cleave mitochondria in a GTPase-dependent manner [1].

Drp1 is a main regulator of mitochondrial fission, and its recruitment to mitochondria is tightly regulated by posttranslational modifications (PTMs) such as phosphorylation, S-nitrosylation, SUMOylation, and ubiquitination [2]. Among these PTMs on Drp1, phosphorylation has been most extensively studied. So far, Drp1 is reported to undergo phosphorylation at serine 616 (S616), serine 637 (S637), and serine 693 (S693). Phosphorylation of Drp1 at different sites causes different effects on the profission activity of Drp1. While Drp1 phosphorylation at S616 and S693 promotes mitochondrial fission, Drp S637 phosphorylation suppresses it [2, 3]. Previous studies have identified multiple kinases that phosphorylate Drp1 at S616. They include

cyclin-dependent kinase 1 (CDK1)/cyclin B1, MAP kinase ERK1/2, protein kinase C  $\delta$  (PKC $\delta$ ), and calmodulin-dependent protein kinase II (CaMKII). CDK1/cyclin B1 mediates mitochondrial fission during mitosis through Drp1 phosphorylation at S616 [4]. ERK1/2 and PKC $\delta$  promote Drp1 S616 phosphorylation and mitochondrial fragmentation under high glucose condition and hypertension encephalopathy, respectively [5, 6]. CaMKII induces Drp1 S616 phosphorylation and mitochondrial fission during chronic  $\beta$ -adrenergic stimulation [7]. Although Drp1 S616 phosphorylation has been shown to be induced by various stimuli, its connection with DNA damage remains uncertain. Recently, Xia and colleagues reported that a chemotherapeutic agent doxorubicin stimulates Drp1 S616 phosphorylation [8], suggesting that genotoxic stress may influence on Drp1 phosphorylation.

Ionizing radiation (IR) elicits various cellular responses including DNA repair, cell cycle arrest, activation of stress signaling, and alteration of mitochondrial function [9, 10]. Thus far, there are several studies reporting the role of mitochondrial dynamics in cellular radioresponses. Kobashigawa *et al.* and Zhang *et al.* showed that  $\gamma$ - and  $\alpha$ -irradiation alter mitochondrial shape via Drp1, respectively [11, 12]. In addition, we reported that Drp1 mediated mitochondrial fission after X-irradiation and its inhibition resulted in the reduction of cellular radiosensitivity and cell death associated with aberrant mitosis [13]. These data indicate that Drp1 participates in mitochondrial dynamics after radiation exposure and plays an important role in determining the fate of irradiated cells. However, it remains unclear how IR promotes Drp1 activation and mitochondrial fission. Here, we provide evidence that Drp1 phosphorylation at S616, but not at S637, is prerequisite for radiation-induced mitochondrial fission and that CaMKII regulates Drp1 phosphorylation at S616 after irradiation.

## **MATERIALS AND METHODS**

### **Reagents**

DH5 $\alpha$ , Phusion® High-Fidelity PCR Kit and MitoTracker Green FM were purchased from Thermo Fisher Scientific (Waltham, MA, USA). U0126, GF109203X and Gö6976 were from EMD Millipore (Billerica, MA, USA). Phorbol 12-myristate 13-acetate (PMA) was from Abcam (Cambridge, MA, USA). KN-93 and KN-92 were obtained from Cayman Chemical (Ann Arbor, MI, USA). The following antibodies were used for Western blotting: anti-Drp1 (BD Biosciences, Billerica, MA, USA), anti-phospho Drp1 S616, anti-phospho Drp1 S637, anti-ERK1/2 and anti-phospho ERK1/2 (Cell Signaling Technology, Beverly, MA, USA), anti-FLAG (Sigma-Aldrich, St. Louis, MO, USA), anti-conventional PKC (cPKC), anti-actin, and HRP-conjugated secondary antibodies (Santa Cruz Biotechnology, Santa Cruz, CA, USA). The Western Lightning Plus-ECL chemiluminescence detection kit was purchased from PerkinElmer (Waltham, MA, USA). Primers were obtained from Integrated DNA Technologies (Coralville, IA, USA).

### **Cell culture and X-irradiation**

The SV40-immortalized MEFs derived from Drp1-deficient mice (KO MEFs) and its control wild-type cells (WT MEFs) were kindly provided by Dr. Masatoshi Nomura (Kyushu University, Fukuoka, Japan) [14] and were maintained in DMEM (Thermo Fisher Scientific) containing 10% (v/v) fetal bovine serum (BD Biosciences) at 37°C in 5% CO<sub>2</sub>. X-irradiation was performed at room temperature using an X-RAD iR-225 X-ray irradiator (Precision X-Ray, North Branford, CT) with a dose rate of 1.37 Gy/min

at 200 kVp and 15 mA with a 1.0-mm aluminum filter. Where necessary, the following inhibitors were used: a MEK1/2 inhibitor, U0126; a PKC inhibitor, GF109203X (GFX); a Ca<sup>2+</sup>-dependent PKC inhibitor, Gö6976 (Gö); a CaMKII inhibitor, KN-93 and its inactive analog, KN-92. When U0126, GFX, and Gö were used, the drugs were applied to WT MEFs 2 h prior to X-irradiation. After irradiation, the medium was replaced with fresh growth medium containing inhibitors and the cells were cultured for analysis. When KN-93 and KN-92 were used, the drugs were applied to WT MEFs immediately after X-irradiation. To deplete PKC, 100 nM PMA was treated for 6 h, followed by X-irradiation. The medium was then replaced with fresh growth medium and the cells were cultured for analysis.

### **Plasmids and transfection**

Mitochondria-targeting roGFP2 plasmid and mCherry-Drp1 plasmid were kindly provided by Prof. James S. Remington (University of Oregon, Oregon, USA) [15] and Prof. Gia K. Voeltz (University of Colorado, Colorado, USA) [16], respectively. To generate a plasmid encoding mitochondria-targeting mCherry, mitochondria-targeting signal derived from human pyruvate dehydrogenase E1 $\alpha$  subunit in mitochondria-targeting roGFP2 plasmid was amplified by PCR and subcloned into pmCherry-N1 (TAKARA BIO INC., Shiga, Japan) using EcoRI. To generate p3 $\times$ FLAG-Drp1 WT plasmid, human Drp1 cDNA in mCherry-Drp1 plasmid was amplified by PCR and subcloned into p3 $\times$ FLAG-CMV7.1 plasmid (Sigma-Aldrich) using NotI/EcoRI. Plasmids of p3 $\times$ FLAG-Drp1 S616A and p3 $\times$ FLAG-Drp1 S637A were generated by PCR-based site-directed mutagenesis using Phusion DNA polymerase. To analyze mitochondrial morphology, plasmids encoding Drp1 and

mitochondria-targeting mCherry were simultaneously introduced into KO MEFs by X-tremeGENE 9 Transfection Reagent (Roche Applied Science, Mannheim, Germany).

### **Mitochondrial morphology**

Cells were seeded on 35-mm glass-bottomed dishes (AGC Techno Glass, Shizuoka, Japan) and cultured overnight. At the times indicated after X-irradiation, the cells were incubated with serum-free medium containing 100 nM MitoTracker Green FM for 30 min at 37°C. After two washes with serum-free medium, fresh growth medium was supplied. Fluorescence images of live cells were obtained using an LSM700 confocal laser scanning microscope (Carl Zeiss, Oberkochen, Germany) at 37°C in 5% CO<sub>2</sub>. The quantitative analysis of mitochondrial morphologies was performed as described previously [13]. Representative images of the different mitochondrial morphologies in each category are shown in Fig. S1. In each experiment, >50 cells/condition were randomly chosen and classified, and the percentage of each category was calculated. Experiments were repeated three times.

### **SDS-PAGE and Western blotting**

Cells were collected and lysed with lysis buffer (50 mM Tris-HCl [pH 7.5], 1% (v/v) Triton X-100, 5% (v/v) glycerol, 5 mM EDTA, and 150 mM NaCl). After centrifugation at 18,000 × g for 15 min at 4°C, supernatants were collected. 3× Laemmli's sample buffer (0.1875 M Tris-HCl [pH 6.8], 15% (v/v) β-mercaptoethanol, 6% (w/v) SDS 30% (v/v) glycerol, and 0.006% (w/v) bromophenol blue) was added to the supernatants, and the samples were boiled for 1 min. Proteins were separated by SDS-PAGE and transferred onto a nitrocellulose membrane (Advantec TOYO, Tokyo,

Japan). The membrane was blocked with TBST (10 mM Tris-HCl [pH 7.4], 0.1 M NaCl, and 0.1% Tween-20) containing 5% (w/v) nonfat skim milk and probed with specific antibodies diluted with TBST containing 5% (w/v) nonfat skim milk or 5% (w/v) BSA overnight at 4°C. After probing with HRP-conjugated secondary antibodies, the bound antibodies were detected with Western Lightning Plus-ECL. Image acquisition was performed with an LAS 4000 mini image analyzer (Fujifilm, Tokyo, Japan), and image analysis was done by MultiGauge software (Fujifilm).

### **Statistical analysis**

All results are expressed as means  $\pm$  SD of at least three separate experiments. Comparison of two groups was performed with Student's *t*-tests. For multiple comparisons, Dunnett's test or Tukey-Kramer test was used. The minimum level of significance was set at  $p < 0.05$ .

## **RESULTS**

### **IR stimulates Drp1 phosphorylation at S616 but not at S637**

To determine whether X-irradiation affects the phosphorylation status of Drp1, we examined Drp1 phosphorylation at S616 and S637 in WT MEFs after exposure to X-rays. As shown in Fig. 1A, 10 Gy X-rays stimulated Drp1 phosphorylation at S616, peaking at 12 h post-irradiation and declining thereafter. On the other hand, phospho-S637 Drp1 was not detectable after 10 Gy irradiation. Furthermore, while Drp1 phosphorylation at S616 was increased in a dose-dependent manner, phospho-S637 Drp1 level was unaffected by X-irradiation at any dose (Fig. 1B). These results demonstrate that IR stimulates Drp1 phosphorylation at S616, but not at S637.

### **Radiation-induced mitochondrial fission is recovered by the introduction of WT and S637A Drp1, but not by S616A Drp1**

In the previous study, we have demonstrated that Drp1 is essential for the radiation-induced mitochondrial fission [13]. This finding prompted us to investigate whether mitochondrial shape change after IR is influenced by the phosphorylation of Drp1. To this end, we prepared the expression plasmids encoding WT Drp1 and phosphorylation-site Drp1 mutants (S616A or S637A Drp1) and transfected them in Drp1-deficient cells to reconstitute Drp1. Transfection of Drp1 constructs in KO MEFs led to the similar levels of protein expression (Fig. 2A). We next evaluated the effect of Drp1 reconstitution on mitochondrial shape. KO MEFs transfected with empty vector had highly networked and elongated mitochondria without or with X-irradiation (Fig. 2B). On the other hand, the cells expressing WT Drp1 had punctate mitochondria after irradiation. Furthermore, mitochondria in S616A Drp1-expressing cells showed tube-like structure and those in S637A Drp1-expressing cells were granulated. To evaluate the mitochondrial morphologies quantitatively, we classified them into four categories (highly connected, tubular, intermediate, and fragmented) by manually analyzing the microscopic images (Fig. 2C and Supplementary Fig. S1). In the vector control cells, IR moderately increased the fraction of the cells with intermediate mitochondria, but the effect of IR on mitochondrial morphologies was ambiguous. In contrast, in WT Drp1-expressing cells, IR caused significant decrease of the cells with highly connected mitochondria and increase of those with fragmented mitochondria. These observations suggest that reconstitution of WT Drp1 was able to restore radiation-induced mitochondrial fission. In S616A Drp1-expressing cells, the impact of

IR on mitochondrial shape was less significant, especially in the fractions of “highly connected” and “fragmented”, than that in WT Drp1-expressing cells. Meanwhile, in S637A Drp1-expressing cells, IR increased the cells with fragmented mitochondria to the equivalent level to those in WT Drp1-expressing cells. These results indicate that Drp1 phosphorylation at S616, but not at S637, is critical for radiation-induced mitochondrial shape change.

### **Inhibition of CaMKII decreases radiation-induced Drp1 phosphorylation at S616**

In search of the kinase responsible for Drp1 S616 phosphorylation after irradiation, we tested various inhibitors of kinases that are previously associated with Drp1 phosphorylation induced by stimuli other than irradiation. [4-7]. First, we examined the involvement of ERK1/2 using a MEK/ERK inhibitor, U0126. While U0126 treatment reduced the phosphorylation level of ERK1/2 in a dose-dependent manner, it was ineffective on Drp1 phosphorylation at S616 (Fig. 3A). When we tested whether PKC phosphorylates Drp1 using two PKC inhibitors, GF109203X and Gö6973, we found that these inhibitors did not influence Drp1 phosphorylation after irradiation (Fig. 3B). We further analyzed the involvement of PKC by depleting PKC using PMA. It has been shown that prolonged PMA treatment downregulates the expression of diacylglycerol-sensitive PKC isoforms, namely, cPKC ( $\alpha$ ,  $\beta$ ,  $\gamma$ ) and novel PKC ( $\delta$ ,  $\epsilon$ ,  $\eta$ ,  $\theta$ ) [17]. As shown in Fig. 3C, although PMA treatment completely abolished the cPKC expression in WT MEFs, it did not alter the level of Drp1 phosphorylation. We then examined the effect of a CaMKII inhibitor, KN-93. KN-93 treatment decreased Drp1 S616 phosphorylation after irradiation in a dose-dependent manner (Fig. 3D). Meanwhile, it was not affected by the treatment of KN-92, an inactive analog of KN-93

(Fig. 3E). These results suggest that CaMKII, but not ERK1/2 or PKC, is involved in radiation-induced Drp1 phosphorylation at S616.

### **Inhibition of CaMKII reduces radiation-induced mitochondrial fission**

To determine the effect of CaMKII inhibition on the radiation-induced mitochondrial fission, we analyzed mitochondrial morphology in WT MEFs treated with KN-93 or KN-92 after irradiation (Fig. 4A, 4B and Supplementary Fig. S3). Mitochondria in untreated cells exhibited networked and tubular shape. IR caused the increase of the cells with fragmented mitochondria and the reduction of those with highly connected as well as tubular mitochondria, as described above. While KN-93 treatment completely canceled the mitochondrial shape change after irradiation, KN-92 treatment did not. These results suggest that CaMKII regulates Drp1 S616 phosphorylation, thereby influencing the radiation-induced mitochondrial fission.

## **DISCUSSION**

In the present study, we showed that Drp1 S616 phosphorylation was an important step for radiation-induced mitochondrial shape change. We observed that X-irradiation at 10 Gy stimulated Drp1 S616 phosphorylation, peaking at 12 h post-irradiation and declining thereafter (Fig. 1A). It is well documented that Drp1 S616 phosphorylation upregulates its activity and promotes Drp1-dependent mitochondrial fission [18]. In fact, this time-course was consistent with the time-course of mitochondrial fission after IR demonstrated in our previous study [13], suggesting that Drp1 S616 phosphorylation plays a role in mitochondrial shape change after irradiation. Furthermore, we revealed that the radiation-induced mitochondrial fission was significantly weaker in S616A

Drp1-expressing cells than in WT Drp1-expressing cells (Fig. 2). This finding corroborates our hypothesis that Drp1 S616 phosphorylation is prerequisite for radiation-induced mitochondrial fission.

Of interest, we observed a partial, not full, recovery of radiation-induced mitochondrial fission by the reconstitution of S616A Drp1 (Fig. 2C). This insufficient recovery implies that X-irradiation activates Drp1 through PTMs other than S616 phosphorylation. At this point, we do not know whether they are the phosphorylation on the other sites or the other types of PTMs. Among various PTMs, SUMOylation could be a potential PTM to modify Drp1 and alter its activity after IR. Previous studies have shown that SUMOylation of Drp1 stabilizes its binding to mitochondria and promotes mitochondrial fission [19]. Together with the evidence that IR induces SUMOylation on several DNA repair proteins [20, 21], it might be possible that IR induces Drp1 SUMOylation and regulates its activity as well as mitochondrial morphology.

In this study, we attempted to identify the kinase responsible for Drp1 S616 phosphorylation after IR, and found that it was regulated by CaMKII. CaMKII is a multifunctional serine/threonine protein kinase and plays important roles in the transmission of Ca<sup>2+</sup> signals to regulate various cellular processes [22]. We observed that pharmacological CaMKII inhibition significantly decreased the radiation-induced Drp1 S616 phosphorylation (Fig. 3D and 3E). In support of this finding, previous studies have reported that CaMKII directly phosphorylates Drp1 at S616 during chronic  $\beta$ -adrenergic stimulation [7] and IR stimulates CaMKII activation in various types of cells [23-25]. These results suggest that CaMKII is responsible for the radiation-induced Drp1 phosphorylation at S616. In addition to the reduction of Drp1 phosphorylation, CaMKII inhibition attenuated mitochondrial shape change after irradiation (Fig. 4). It

corroborates the presence of signaling mechanism by which CaMKII activation after IR stimulates Drp1 S616 phosphorylation, leading to mitochondrial fission.

In conclusion, we investigated the molecular mechanism by which IR activates Drp1 and induces mitochondrial fission. It was demonstrated that Drp1 phosphorylation at S616, but not at S637, is prerequisite for radiation-induced mitochondrial shape change and that CaMKII regulates Drp1 phosphorylation, thereby influencing on the radiation-induced mitochondrial fission. We believe that our findings in this study contribute to understand the role of mitochondrial dynamics in cellular radioresponse.

#### **CONFLICT OF INTEREST**

The authors declare no conflict of interest.

#### **ACKNOWLEDGEMENTS**

We are deeply grateful to Dr. Masatoshi Nomura for generously providing MEFs. We appreciate Prof. James S. Remington and Prof. Gia K. Voeltz for kindly providing plasmids. We would like to thank Editage ([www.editage.jp](http://www.editage.jp)) for English language editing.

#### **FUNDING**

This work was supported, in part, by the JSPS KAKENHI (Grant Numbers 16J03822 [YS], 26461875, 17K10465 [TY], 17H03920 [OI]). YS was supported by a JSPS Research Fellowship for Young Scientists. The sponsors had no role in the study design; in the collection, analysis, and interpretation of data; in the writing of the manuscript;

nor the decision to submit the manuscript for publication.

## REFERENCES

- [1] S. Hoppins, L. Lackner, J. Nunnari, The machines that divide and fuse mitochondria, *Annu Rev Biochem*, 76 (2007) 751-780.
- [2] H. Otera, N. Ishihara, K. Mihara, New insights into the function and regulation of mitochondrial fission, *Biochim Biophys Acta*, 1833 (2013) 1256-1268.
- [3] C.H. Chou, C.C. Lin, M.C. Yang, C.C. Wei, H.D. Liao, R.C. Lin, W.Y. Tu, T.C. Kao, C.M. Hsu, J.T. Cheng, A.K. Chou, C.I. Lee, J.K. Loh, S.L. Howng, Y.R. Hong, GSK3beta-mediated Drp1 phosphorylation induced elongated mitochondrial morphology against oxidative stress, *PLoS One*, 7 (2012) e49112.
- [4] N. Taguchi, N. Ishihara, A. Jofuku, T. Oka, K. Mihara, Mitotic phosphorylation of dynamin-related GTPase Drp1 participates in mitochondrial fission, *J Biol Chem*, 282 (2007) 11521-11529.
- [5] T. Yu, B. Jhun, Y. Yoon, High-Glucose Stimulation Increases Reactive Oxygen Species Production Through the Calcium and Mitogen-Activated Protein Kinase-Mediated Activation of Mitochondrial Fission, *Antioxid Redox Signal*, 14 (2011) 425-437.
- [6] X. Qi, M.H. Disatnik, N. Shen, R.A. Sobel, D. Mochly-Rosen, Aberrant mitochondrial fission in neurons induced by protein kinase C $\{\delta\}$  under oxidative stress conditions in vivo, *Mol Biol Cell*, 22 (2011) 256-265.
- [7] S. Xu, P. Wang, H. Zhang, G. Gong, N. Gutierrez Cortes, W. Zhu, Y. Yoon, R. Tian, W. Wang, CaMKII induces permeability transition through Drp1 phosphorylation during chronic beta-AR stimulation, *Nat Commun*, 7 (2016) 13189.

- [8] Y. Xia, Z. Chen, A. Chen, M. Fu, Z. Dong, K. Hu, X. Yang, Y. Zou, A. Sun, J. Qian, J. Ge, LCZ696 improves cardiac function via alleviating Drp1-mediated mitochondrial dysfunction in mice with doxorubicin-induced dilated cardiomyopathy, *J Mol Cell Cardiol*, 108 (2017) 138-148.
- [9] D. Eriksson, T. Stigbrand, Radiation-induced cell death mechanisms, *Tumour Biol*, 31 (2010) 363-372.
- [10] S.P. Jackson, J. Bartek, The DNA-damage response in human biology and disease, *Nature*, 461 (2009) 1071-1078.
- [11] B. Zhang, M.M. Davidson, H. Zhou, C. Wang, W.F. Walker, T.K. Hei, Cytoplasmic irradiation results in mitochondrial dysfunction and DRP1-dependent mitochondrial fission, *Cancer Res*, 73 (2013) 6700-6710.
- [12] S. Kobashigawa, K. Suzuki, S. Yamashita, Ionizing radiation accelerates Drp1-dependent mitochondrial fission, which involves delayed mitochondrial reactive oxygen species production in normal human fibroblast-like cells, *Biochem Biophys Res Commun*, 414 (2011) 795-800.
- [13] T. Yamamori, S. Ike, T. Bo, T. Sasagawa, Y. Sakai, M. Suzuki, K. Yamamoto, M. Nagane, H. Yasui, O. Inanami, Inhibition of the mitochondrial fission protein dynamin-related protein 1 (Drp1) impairs mitochondrial fission and mitotic catastrophe after x-irradiation, *Mol Biol Cell*, 26 (2015) 4607-4617.
- [14] N. Ishihara, M. Nomura, A. Jofuku, H. Kato, S.O. Suzuki, K. Masuda, H. Otera, Y. Nakanishi, I. Nonaka, Y. Goto, N. Taguchi, H. Morinaga, M. Maeda, R. Takayanagi, S. Yokota, K. Mihara, Mitochondrial fission factor Drp1 is essential for embryonic development and synapse formation in mice, *Nat Cell Biol*, 11 (2009) 958-966.
- [15] G.T. Hanson, R. Aggeler, D. Oglesbee, M. Cannon, R.A. Capaldi, R.Y. Tsien, S.J.

Remington, Investigating mitochondrial redox potential with redox-sensitive green fluorescent protein indicators, *J Biol Chem*, 279 (2004) 13044-13053.

[16] J.R. Friedman, L.L. Lackner, M. West, J.R. DiBenedetto, J. Nunnari, G.K. Voeltz, ER tubules mark sites of mitochondrial division, *Science*, 334 (2011) 358-362.

[17] B. Marengo, C. De Ciucis, R. Ricciarelli, M.A. Pronzato, U.M. Marinari, C. Domenicotti, Protein kinase C: an attractive target for cancer therapy, *Cancers (Basel)*, 3 (2011) 531-567.

[18] S.L. Archer, Mitochondrial dynamics--mitochondrial fission and fusion in human diseases, *N Engl J Med*, 369 (2013) 2236-2251.

[19] J. Prudent, R. Zunino, A. Sugiura, S. Mattie, G.C. Shore, H.M. McBride, MAPL SUMOylation of Drp1 Stabilizes an ER/Mitochondrial Platform Required for Cell Death, *Mol Cell*, 59 (2015) 941-955.

[20] Y. Galanty, R. Belotserkovskaya, J. Coates, S. Polo, K.M. Miller, S.P. Jackson, Mammalian SUMO E3-ligases PIAS1 and PIAS4 promote responses to DNA double-strand breaks, *Nature*, 462 (2009) 935-939.

[21] H. Shima, H. Suzuki, J. Sun, K. Kono, L. Shi, A. Kinomura, Y. Horikoshi, T. Ikura, M. Ikura, R. Kanaar, K. Igarashi, H. Saitoh, H. Kurumizaka, S. Tashiro, Activation of the SUMO modification system is required for the accumulation of RAD51 at sites of DNA damage, *J Cell Sci*, 126 (2013) 5284-5292.

[22] G. Manning, D.B. Whyte, R. Martinez, T. Hunter, S. Sudarsanam, The protein kinase complement of the human genome., *Science*, 298 (2002) 1912-1934.

[23] D. Palme, M. Misovic, E. Schmid, D. Klumpp, H.R. Salih, J. Rudner, S.M. Huber, Kv3.4 potassium channel-mediated electrosignaling controls cell cycle and survival of irradiated leukemia cells, *Pflugers Arch*, 465 (2013) 1209-1221.

- [24] L. Enns, D. Murray, R. Mizayans, Effects of the protein kinase inhibitors wortmannin and KN62 on cellular radiosensitivity and radiation-activated S phase and G1/S checkpoints in normal human fibroblasts, *Br J Cancer*, 6 (1999) 959-965.
- [25] C. Sag, H. Wolff, K. Neumann, M. Opiela, J. Zhang, F. Steuer, T. Sowa, S. Gupta, M. Schirmer, M. Hünlich, M. Rave-Fränk, C. Hess, M. Anderson, A. Shah, H. Christiansen, L. Maier, Ionizing radiation regulates cardiac Ca handling via increased ROS and activated CaMKII, *Basic Res Cardiol.*, 6 (2013) 385.

## FIGURE LEGENDS

**Fig. 1.** IR stimulates Drp1 phosphorylation at S616 but not S637. (A) WT MEF cells were collected at the indicated times after X-irradiation at 10 Gy. Top, representative blots of phospho-S616, phospho-S637 and total Drp1. Arrowheads denote the positions of the bands corresponding to phospho-S637 Drp1. Bottom, time-course analysis of Drp1 phosphorylation at S616. The intensities of phospho-S616 Drp1 bands were normalized to those of total Drp1 bands. Data are expressed as means  $\pm$  SD of three experiments.  $*p < 0.05$  and  $**p < 0.01$  vs. 0 h (Dunnett's test). (B) WT MEF cells were collected at 12 h after X-irradiation at the indicated doses. Top, representative blots of phospho-S616, phospho-S637 and total Drp1. Arrowheads denote the positions of the bands corresponding to phospho-S637 Drp1. Bottom, dose-response analysis of Drp1 phosphorylation at S616. Data are expressed as means  $\pm$  SD of three experiments.  $*p < 0.05$  and  $**p < 0.01$  vs. 0 Gy (Dunnett's test).

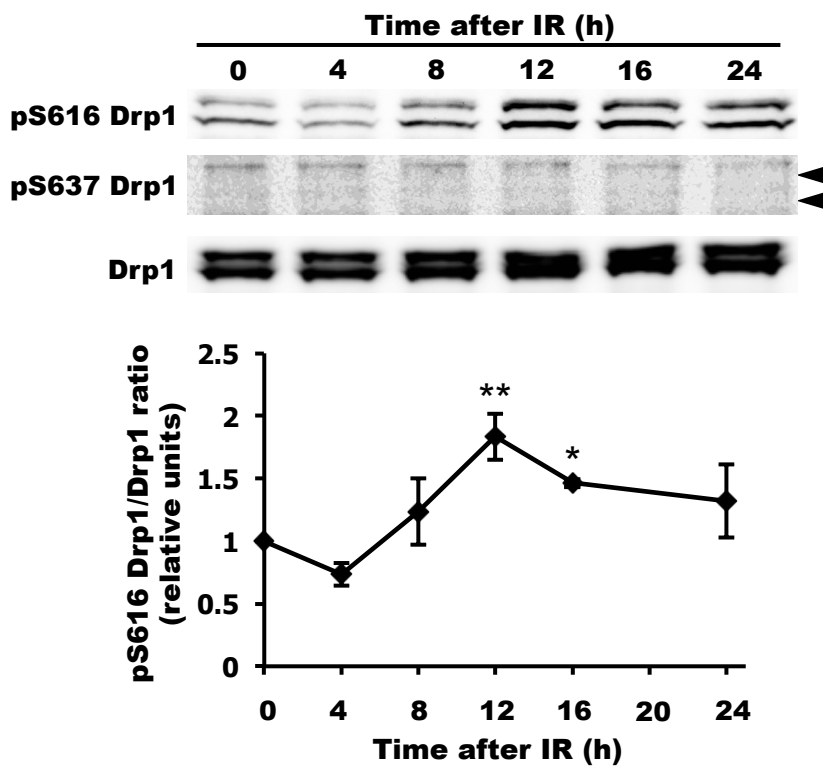
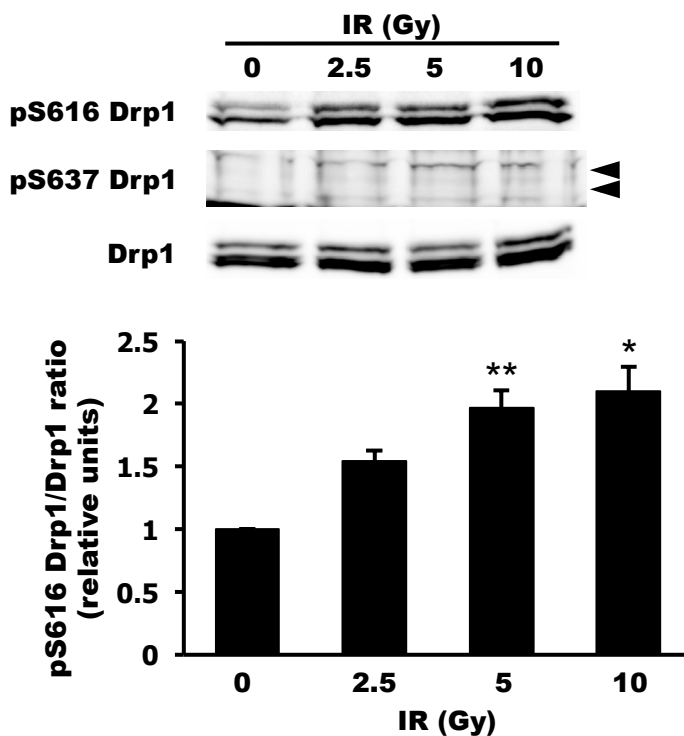
**Fig. 2.** Radiation-induced mitochondrial fission is recovered by the introduction of WT and S637A Drp1, but not by S616A Drp1. (A) Drp1 KO MEFs were transiently transfected with plasmids encoding 3xFLAG-tagged wild-type Drp1 (WT), Drp1 S616A (S616A), Drp1 S637A (S637A) or empty vector (Vec). After 24-h incubation, the expression levels of exogenous Drp1 were analyzed by Western blotting. Representative blots of FLAG and actin are shown. (B and C) To analyze mitochondrial morphology, plasmids encoding Drp1 and mitochondria-targeting mCherry were simultaneously introduced into KO MEFs. After 24-h incubation, the cells were X-irradiated at 10 Gy and incubated for 8 h. Mitochondrial morphology was analyzed by confocal laser scanning microscopy. (B) Representative confocal images of mitochondria in the cells.

Bottom, magnified images of boxed region. (C) Quantitative image analysis of mitochondrial morphologies. Data are expressed as means  $\pm$  SD of three experiments.

**Fig. 3.** Inhibition of CaMKII decreases radiation-induced Drp1 S616 phosphorylation. (A) WT MEFs were X-irradiated at 10 Gy in the presence or absence of U0126. After incubation for 12 h, the phosphorylation and expression of Drp1 and ERK1/2 were analyzed by Western blotting. (B) WT MEFs were X-irradiated at 10 Gy in the presence or absence of GF102903X (GFX) or Gö6976 (Gö). After incubation for 12 h, the phosphorylation and expression of Drp1 were analyzed by Western blotting. (C) WT MEFs were treated with 100 nM PMA for 6 h before X-irradiation. After X-irradiation at 10 Gy, the cells were incubated for 12 h and collected. The phosphorylation and expression of Drp1 and cPKC were analyzed by Western blotting. (D and E) WT MEFs were X-irradiated at 10 Gy and treated with KN-93 (D) or KN-92 (E). After the cells were collected at the indicated times, the phosphorylation and expression of Drp1 were analyzed by Western blotting. Top, representative blots of phospho-S616 Drp1 and total Drp1. Bottom, The levels of Drp1 phosphorylation at S616 were quantified relative to that of control. Data are expressed as means  $\pm$  SD of three experiments. \* $p < 0.05$  and \*\* $p < 0.01$  vs. 0 nM KN-93 (Student's *t*-test).

**Fig. 4.** Inhibition of CaMKII reduces radiation-induced mitochondrial fission. (A and B) After X-irradiation at 10 Gy, WT MEFs were treated with 100 nM KN-92 or KN-93 and incubated for 12 h. Mitochondria were stained with MitoTracker Green FM and analyzed. (A) Representative confocal images of mitochondria in the cells. Bottom,

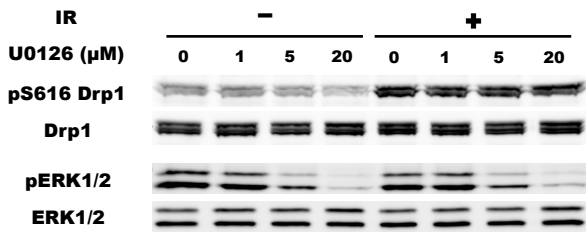
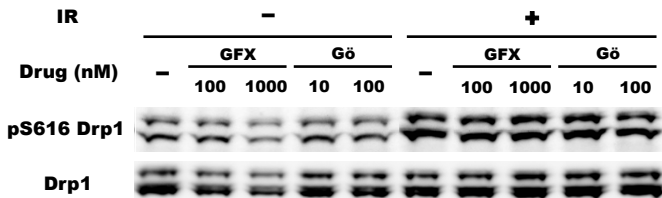
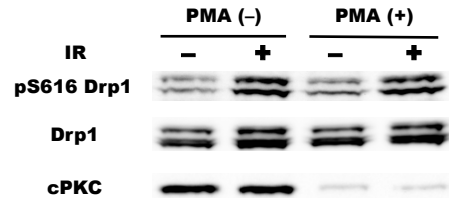
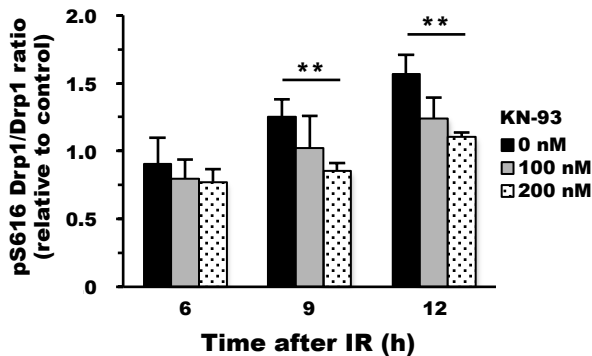
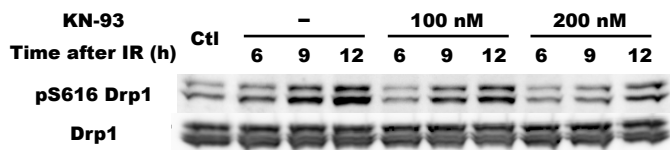
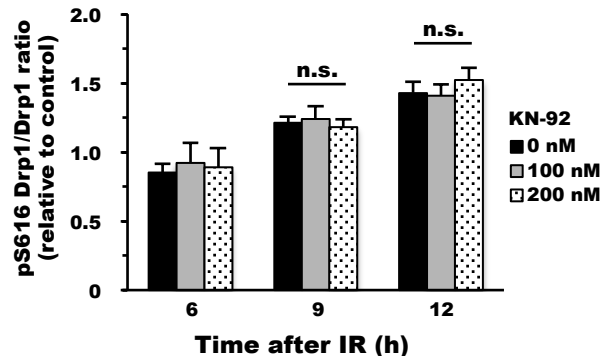
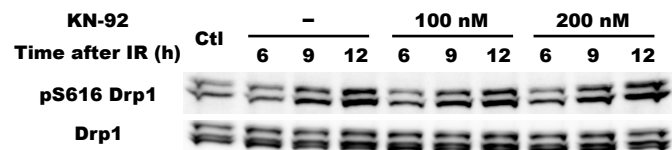
magnified images of boxed region. (B) Quantitative image analysis of mitochondrial morphologies. Data are expressed as means  $\pm$  SD of three experiments.

**A****B**

### Figure 1: IR stimulates Drp1 phosphorylation at S616 but not S637.

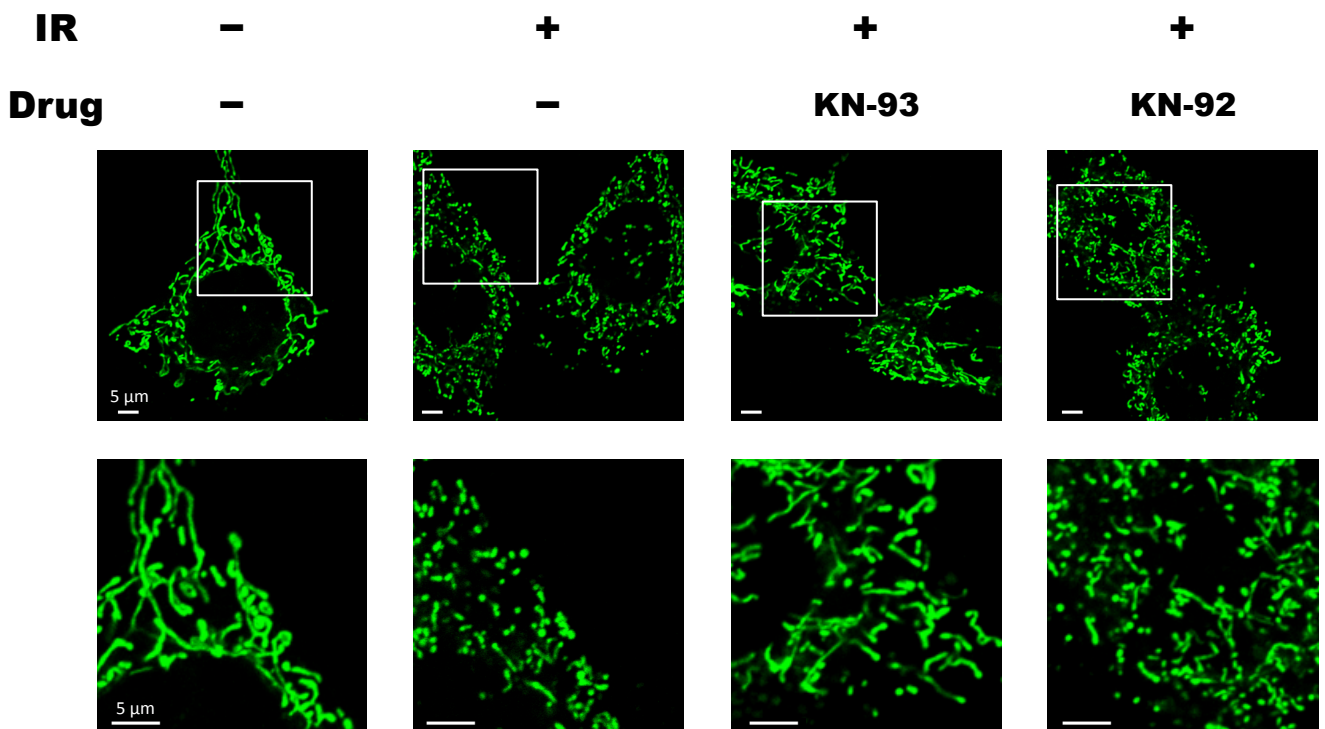
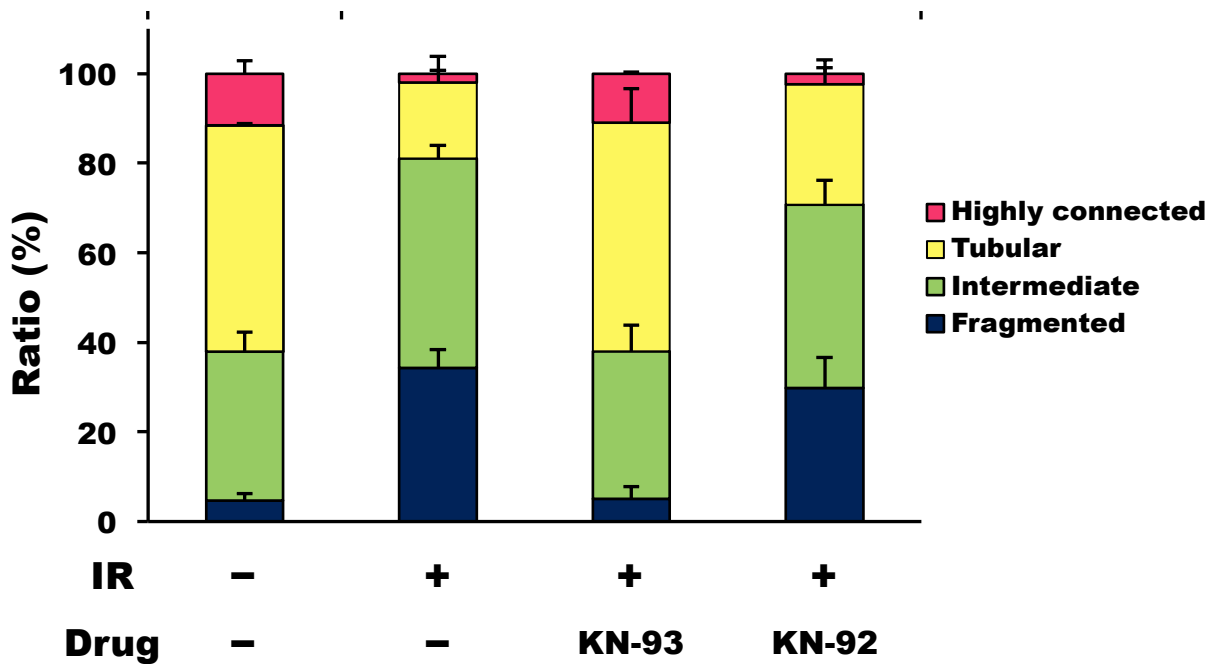
(A) WT MEF cells were collected at the indicated times after X-irradiation at 10 Gy. The phosphorylation and expression of Drp1 were analyzed by Western blotting. Top, representative blots of phospho-S616, phospho-S637 and total Drp1. Arrowheads denote the positions of the bands corresponding to phospho-S637 Drp1. Bottom, time-course analysis of Drp1 phosphorylation at S616. The intensities of phospho-S616 Drp1 bands were normalized to those of total Drp1 bands. Data are expressed as means  $\pm$  SD of three experiments. \* $p < 0.05$  and \*\* $p < 0.01$  vs. 0 h (Dunnett's test). (B) WT MEF cells were collected at 12 h after X-irradiation at the indicated doses. The phosphorylation and expression of Drp1 were analyzed by Western blotting. Top, representative blots of phospho-S616, phospho-S637 and total Drp1. Arrowheads denote the positions of the bands corresponding to phospho-S637 Drp1. Bottom, dose-response analysis of Drp1 phosphorylation at S616. Data are expressed as means  $\pm$  SD of three experiments. \* $p < 0.05$  and \*\* $p < 0.01$  vs. 0 Gy (Dunnett's test).



**A****B****C****D****E**

**Figure 3: Inhibition of CaMKII decreases radiation-induced Drp1 phosphorylation at S616.**

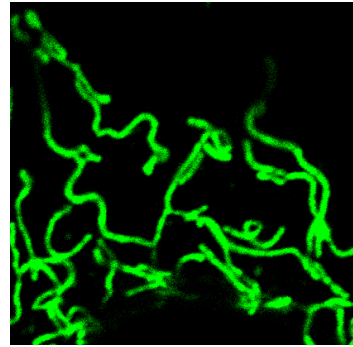
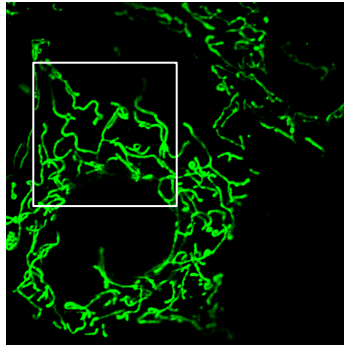
(A) Effect of a MEK inhibitor on radiation-induced Drp1 phosphorylation at S616. WT MEFs were X-irradiated at 10 Gy in the presence or absence of U0126. After incubation for 12 h, the cells were collected. The phosphorylation and expression of Drp1 and ERK1/2 were analyzed by Western blotting. (B and C) Effect of PKC inhibitor treatment or PKC-depletion on radiation-induced Drp1 phosphorylation at S616. (B) WT MEFs were X-irradiated at 10 Gy in the presence or absence of GF102903X (GFX) or Gö6976 (Gö). After incubation for 12 h, the cells were collected. The phosphorylation and expression of Drp1 were analyzed by Western blotting. (C) WT MEFs were treated with 100 nM PMA for 6 h before X-irradiation. After X-irradiation at 10 Gy, the cells were incubated for 12 h and collected. The phosphorylation and expression of Drp1 and cPKC were analyzed by Western blotting. (D and E) Effect of a CaMKII inhibitor on radiation-induced Drp1 phosphorylation at S616. WT MEFs were X-irradiated at 10 Gy and treated with KN-93 (D) or KN-92 (E). The cells were collected at the indicated times. The phosphorylation and expression of Drp1 were analyzed by Western blotting. Top, representative blots of phospho-S616 Drp1 and total Drp1. Bottom, The levels of Drp1 phosphorylation at S616 were quantified relative to that of control. Data are expressed as means  $\pm$  SD of three experiments. \* $p < 0.05$  and \*\* $p < 0.01$  vs. 0 nM KN-93 (Student's t test).

**A****B**

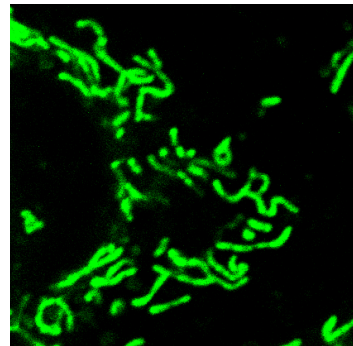
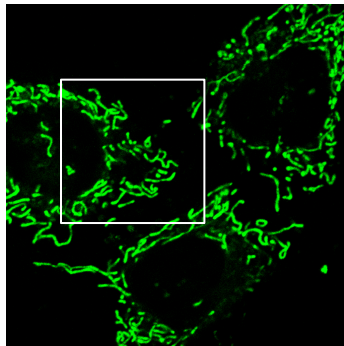
**Figure 4: Inhibition of CaMKII reduces radiation-induced mitochondrial fission.**

(A and B) After X-irradiation at 10 Gy, WT MEFs were treated with 100 nM KN-92 or KN-93 and incubated for 12 h. Mitochondria were stained with MitoTracker Green FM and analyzed. (A) Representative confocal images of mitochondria in the cells. Bottom, magnified images of boxed region. (B) Quantitative image analysis of mitochondrial morphologies. Data are expressed as means  $\pm$  SD of three experiments.

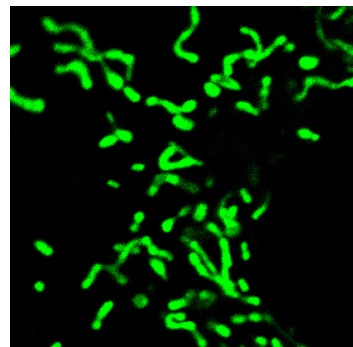
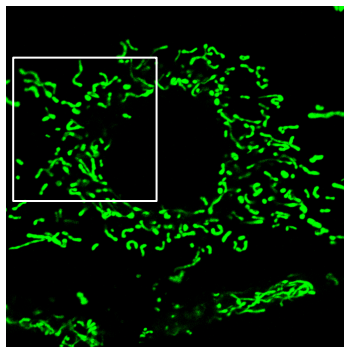
**Highly connected**



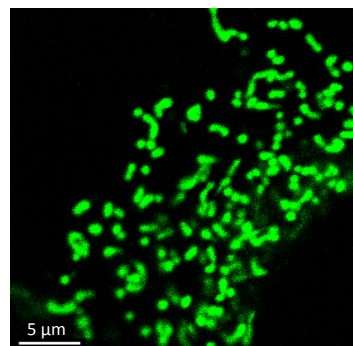
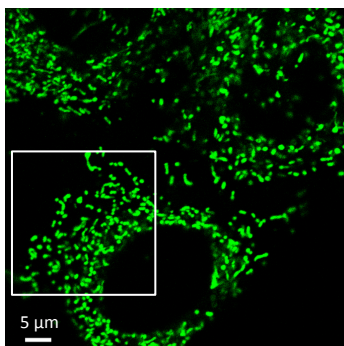
**Tubular**



**Intermediate**

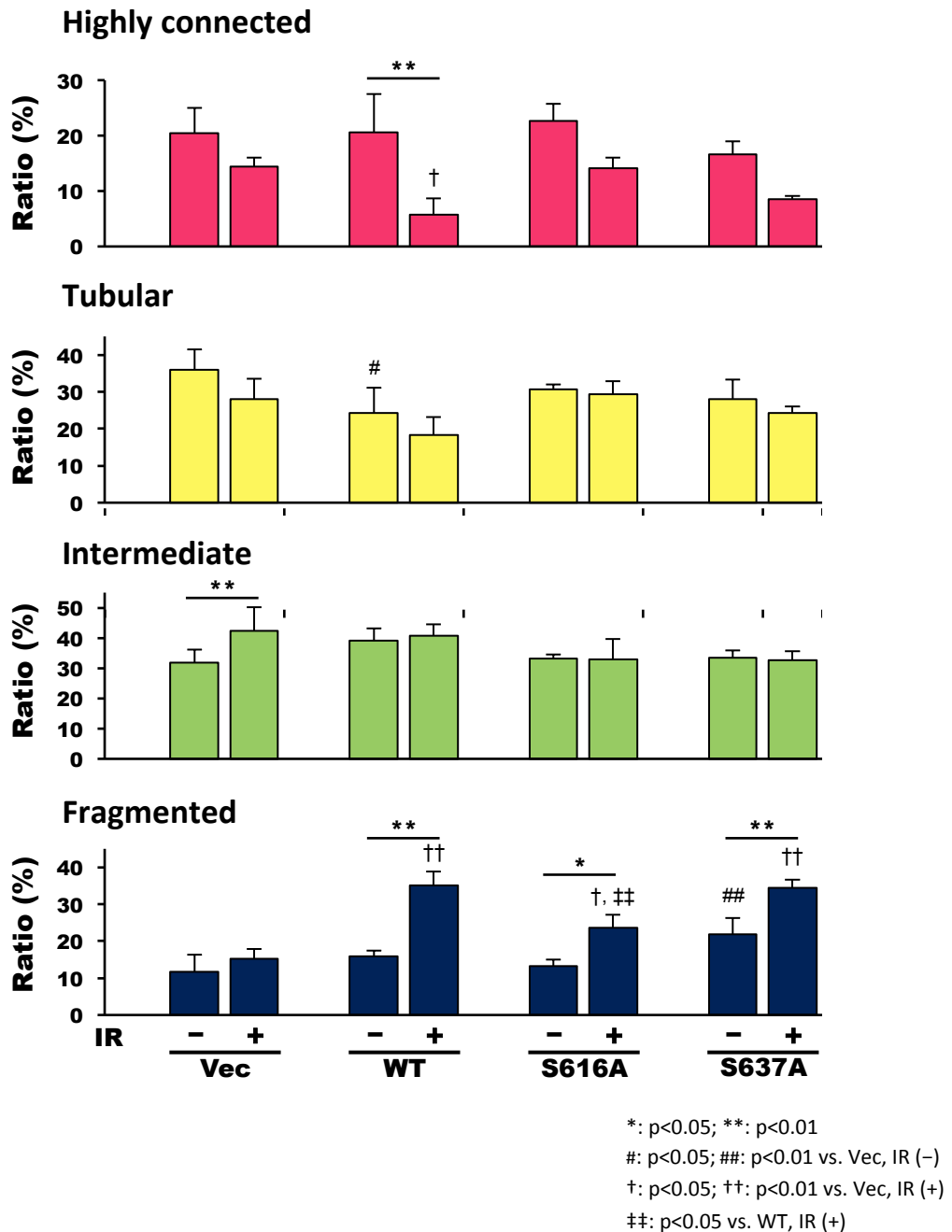


**Fragmented**



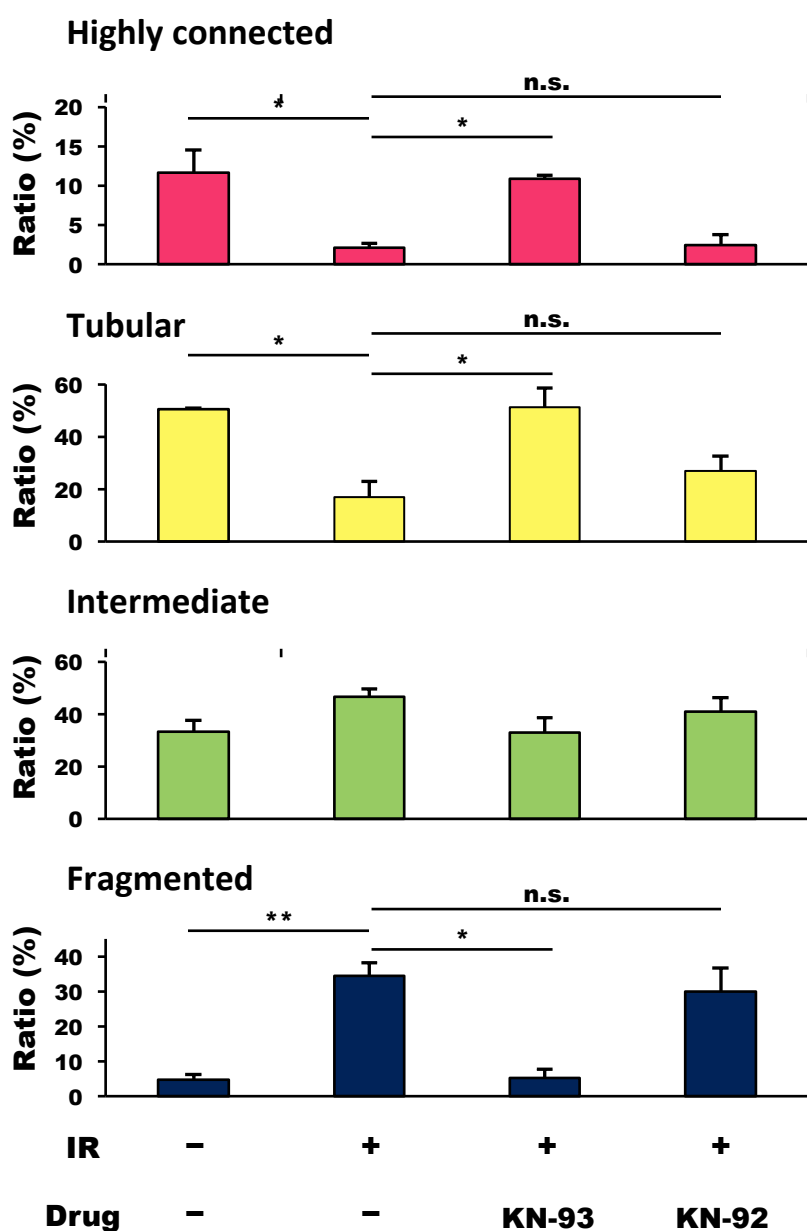
**Supplementary Figure 1. Representative mitochondrial morphologies.**

Mitochondrial morphologies were classified as highly connected, tubular, intermediate, and fragmented, as described in materials and methods. (left) Representative images of mitochondrial morphologies at a low magnification. (right) Magnified images of the boxed regions.



**Supplementary Figure 2. Statistical analysis of mitochondrial morphologies.**

(A) Statistical analysis of the data shown in Figure 2C. Data are expressed as means  $\pm$  SD of three experiments. \*: p<0.05; \*\*: p<0.01, #: p<0.05; ##: p<0.01 vs. Vec, IR (-), †: p<0.05; ††: p<0.01 vs. Vec, IR (+), ‡‡: p<0.01 vs. WT, IR (+) (Tukey-Kramer test).



**Supplementary Figure 3. Statistical analysis of mitochondrial morphologies.**

(A) Statistical analysis of the data shown in Figure 4B. Data are expressed as means  $\pm$  SD of three experiments. \*:  $p < 0.05$ ; \*\*:  $p < 0.01$  (Tukey-Kramer test). n.s.; not significant.